



## $T_g$ and reactivity at the nanoscale

Yung P. Koh, Qingxiu Li, Sindee L. Simon\*

Department of Chemical Engineering, Texas Tech University, Lubbock, TX 79409, United States

### ARTICLE INFO

#### Article history:

Available online 17 June 2009

#### Keywords:

Nanoconfinement  
Reactivity  
Glass transition temperature ( $T_g$ )  
Controlled pore glass  
Differential scanning calorimetry (DSC)

### ABSTRACT

Nanoscale constraint is known to have a significant impact on the thermal properties of materials. In this work, differential scanning calorimetry (DSC) is used to investigate the depression in the glass transition temperature ( $T_g$ ) and the reactivity of a monofunctional and of a difunctional cyanate ester cured under nanoscale constraint. Both reactants undergo trimerization, but the former forms a small molecular-weight compound, whereas the latter forms a polycyanurate network material. A  $T_g$  depression is observed for both the reactants and their products; the magnitude of the depression seems to be related to the size of the molecule being confined relative to the confinement size. The trimerization reaction is accelerated relative to the bulk when the reactants are confined in nanopores. This is clearly observed by a shift in the reaction exotherms to lower temperatures for dynamic temperature scans. Quantification of the acceleration is accomplished by converting the dynamic temperature scan data to conversion versus time data assuming constant activation energy. The results are consistent with acceleration factors obtained from isothermal cure studies, but the dynamic data is considerably easier to obtain.

© 2009 Elsevier B.V. All rights reserved.

### 1. Introduction

Since the pioneering work by Jackson and McKenna in the early 1990s, [1,2] numerous studies have reported that the thermal properties of materials are affected under nanoscale constraint [3–11]. The behavior of low-molecular-weight and polymeric glass formers confined in nanoporous matrices has been extensively examined [2–10] and the general observation is that of a depression in the glass transition temperature ( $T_g$ ) except when strong surface interactions dominate. In polystyrene confined to ultrathin films, a clear molecular weight effect is observed for molecular weights greater than 200 kg/mol, [11] but the effect of molecular size relative to confinement size has not been thoroughly studied for materials confined in nanopores. Work was performed by Schönhals et al. [12] in which the  $T_g$  depression for propylene glycol and oligomeric polypropylene glycol were compared, but in that work, the response of the  $T_g$  depression in oligo-propylene glycol is only a few degrees, whereas for propylene glycol, the response is dominated by absorption, with no evidence of a  $T_g$  depression at any pore size and only a 4 K increase in the smallest 2.5 nm diameter pores. In this work we explore the influence of molecular size on nanoconfinement effects by studying the  $T_g$  depression of four nanoconfined materials: a monofunctional cyanate ester, a difunctional cyanate ester, and the reaction products of these two materials: a low-molecular

weight triazine compound and a crosslinked polycyanurate network, respectively.

In addition to examining the  $T_g$  depression, we are also interested in reactivity at the nanoscale. In prior studies [13,14] we showed that the reactivity of difunctional cyanate ester was enhanced when confined in both silanized and native nanopores. Although the enhancement in native nanopores is partially attributable to the presence of catalytic hydroxyl groups on the nanopore surface, the enhancement in silanized pores was hypothesized to be due to an enhanced collision frequency: functional groups are more likely to react in the smaller pore size due to a decreased ability to diffuse apart prior to reaction because of the presence of a nearby surface. [13,14] In this work, we compare the enhanced reactivity of monofunctional and difunctional cyanate esters.

An understanding of changes in  $T_g$  at the nanoscale is important from both fundamental and practical points of view since  $T_g$  is one of the most important properties for determining upper use temperatures and properties of amorphous materials. Similarly, changes in reactivity under nanoconstraints are important from both fundamental and practical perspectives. Furthermore, these changes, both in properties and reactivity, are not only relevant to reactants confined in nanopores, but may also be relevant to, for example, thermosetting resins cured in the presence of nanoparticles or nanotubes. In fact, close relevance has been suggested to exist between nanofilled polymers and ultrathin films with the spacing between particles dominating the response in nanofilled systems and the smallest dimension dominating the properties in ultrathin films [15–18]. However, the similarity in the quantitative relationship

\* Corresponding author.

E-mail address: [Sindee.Simon@ttu.edu](mailto:Sindee.Simon@ttu.edu) (S.L. Simon).

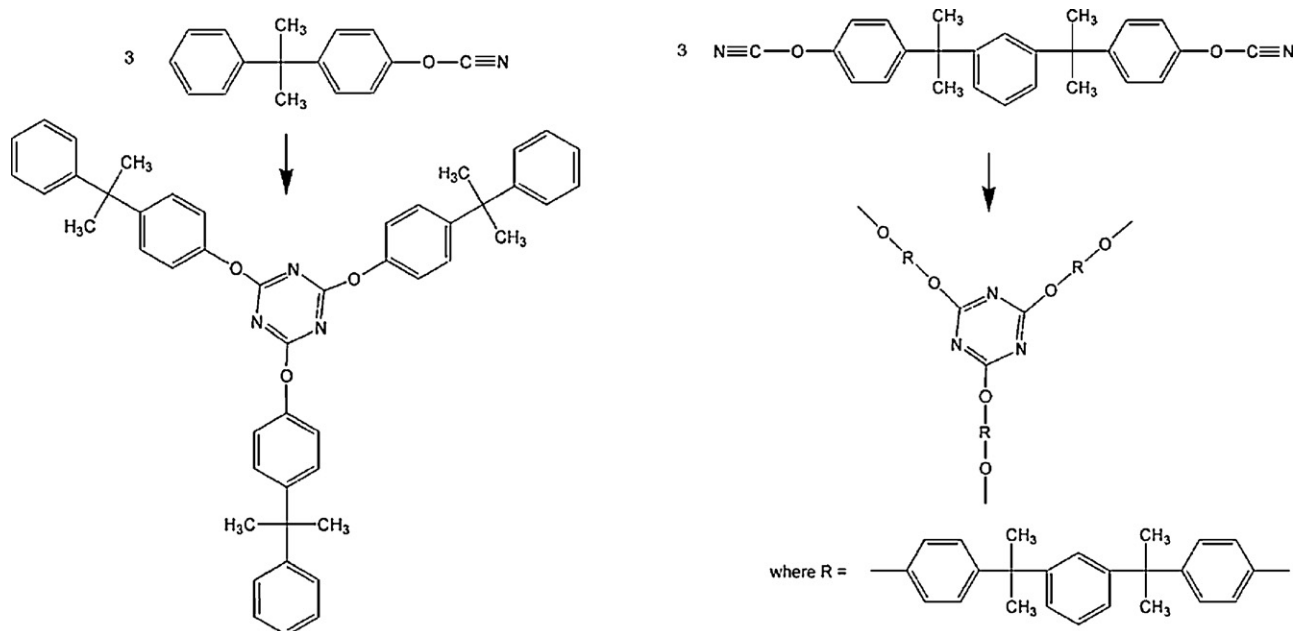


**Fig. 1.** Chemical structure of monofunctional 4-cumylphenol cyanate ester (at left top), difunctional bisphenol M dicyanate ester (at right top), and their respective reaction products.

between  $T_g$  and length scale in the two systems has been questioned [19]. In addition, there may be competing effects in the nanofilled system; in particular, strong interactions between nanofillers and their matrices may dominate changes in properties and reactivity in such systems. We suggest that reaction in nanopores, where interactions can be more easily modified, is ideal for studying how confinement size influences reactivity.

## 2. Experimental methodology

### 2.1. Materials

Two cyanate ester reactants are compared in this work, monocyanate ester, 4-cumylphenol cyanate ester (Oakwood products) and bisphenol M dicyanate ester (BMDC, trade name RTX-84921 from Hi-Tek Polymers, Louisville, KY). Both cyanate esters are used as received. The chemical structures of the materials are shown in Fig. 1a and b; their nominal molar masses are 237 and 396 g/mol, respectively. Three cyanate ester functional groups react to form a cyanurate or triazine ring, as also shown in Fig. 1. The reaction product of the monofunctional material is its trimer with a molar mass of 712 g/mol, whereas the reaction product of the difunctional reactant is crosslinked (infinite molecular weight).

The nanoconfinement mediums used are controlled pore glasses (CPGs, produced from borosilicate glass by Millipore, Billerica, MA) with pore sizes ranging from 8.1 to 287.8 nm. The controlled pore glasses have a mesh size of 120/200 or 74–125  $\mu\text{m}$  and the bulk density of the particles are approximately 300 g/L as provided by the manufacturer. The specifications of the controlled pore glasses listed in Table 1 are also as provided by the manufacturer. To eliminate the effect of hydroxyl groups on the CPG surfaces, the controlled pore glasses were treated as follows: the raw controlled pore glasses were first cleaned by immersing in 69.7% nitric acid at approximately 100 °C for 10 h, rinsed well with distilled water, and dried at 285 °C for 24 h under vacuum. The cleaned controlled pore glasses were then derivatized with hexamethyldisilazane to convert the surface hydroxyl groups to trimethylsilyl groups following the procedure reported in the literature. [1] The silanization treatment has been reported to not significantly affect the pore

size. [20] The silanized CPGs are stored in a desiccator before use.

The cyanate ester reactants are imbibed into the nanopores of controlled pore glass by capillary forces. For the monofunctional material, this is accomplished at room temperature. For the difunctional material, it is accomplished at 100 °C, above its melting temperature of 68 °C. Imbibement occurs in a matter of minutes, consistent with theoretical analysis by Huber et al. [21] and because we use only neat reactants (without catalyst), the imbibement occurs without a significant degree of curing.

A Mettler-Toledo differential scanning calorimeter DSC823e with a Julabo FT100 intracooler and nitrogen purge gas was used for calorimetric measurements of the difunctional cyanate ester, whereas a PerkinElmer Pyris 1 DSC with an intracooler, maintained at –85 °C, was used for most measurements of the monofunctional cyanate ester. Due to the low  $T_g$  of the unreacted monofunctional cyanate ester, however, a Mettler Toledo DSC1 equipped with a liquid nitrogen cooling system, was used for those measurements. Controlled pore glass with weight ranging from 2 to 21 mg was loaded into DSC pans followed by the 4 to 12 mg of reactant. The controlled pore glasses are all underfilled and the fullness ranges from 50% to 98% based on the manufacturer-reported pore volumes. The glass transition temperature is found to be the same, within the error of the measurements, independent of degree of pore fullness for the materials studied. [13] We found that the  $T_g$  and heat of reaction are independent of both the degree of pore fullness and sample size; similar results have been reported [22] for  $T_g$  of hydrogen-bonding liquids in silanized pores. The DSC pans were sealed under nitrogen atmosphere. The temperature of the DSC was calibrated at 10 K/min on heating with mercury and indium for the dicyanate ester studies, and with these standards and n-octane for the monocyanate ester studies. The DSC temperature was maintained at an accuracy of  $\pm 0.1$  °C. The heat flow of the DSC was calibrated with indium.

The glass transition temperature is used in this work to follow the reaction since it is well known that cyanate esters show a unique one-to-one relationship between  $T_g$  and conversion. Heating curves made after curing for a designated time and cooling at a given rate are made and are analyzed to give the limiting fic-

**Table 1**  
Specifications of controlled pore glasses.

Product name	Mean pore diameter (nm) <sup>a</sup>	Pore diameter distribution (%) <sup>b</sup>	Specific pore volume (cm <sup>3</sup> /g) <sup>a</sup>	Specific surface area (m <sup>2</sup> /g) <sup>c</sup>
CPG00080	8.1	9.0	0.49	197.0
CPG00110	11.5	7.3	0.49	119.5
CPG00130	13.0	7.4	0.68	130.0
CPG00240	24.6	7.7	0.83	79.6
CPG00500	50.0	3.7	1.10	50.9
CPG01000	110.6	3.6	1.06	25.0
CPG01200	122.1	3.7	1.73	31.2
CPG3000	287.8	5.3	1.06	8.6

<sup>a</sup> Determined by mercury intrusion method.

<sup>b</sup> Analyzed by ultrasonic sieving method

<sup>c</sup> Measured by nitrogen adsorption method

tive temperature ( $T_f$ ) by the method proposed by Moynihan and co-workers [23,24]. Although  $T_f$  is measured, we call this value the glass transition temperature in the remainder of the text since  $T_f$  is approximately equal (within  $\sim 1$  K) to the glass transition temperature that would be obtained on cooling at the same rate [25–27]. In addition to  $T_g$ , the reaction exotherm of the initially uncured materials is measured at a rate of 10 K/min. For the calculation of the heat of reaction, a sigmoidal baseline was used. As discussed later, the heats of reaction are not a function of either the functionality or the pore size in this system indicating that full conversion is achieved. This also suggests that the chemical structure of the network is not affected by nanoconfinement; however, our result is in contrast to the finding from Kim and Torkelson, which shows that nanoconfinement reduces the physical crosslinking and network formation in a telechelic, pyrene-labeled poly(dimethylsiloxane) thin film system. [28]

### 3. Results

#### 3.1. The glass transition temperature under nanoconfinement

The depression of the glass transition temperatures for the two reactants and their respective reaction products (at full conversion) as a function of reciprocal pore size is shown in Fig. 2. Although the bulk materials only show one  $T_g$  value, at the nanoscale, two glass transition temperatures are observed for the monocyanate ester

and its trimer in all pore sizes, as well for the dicyanate ester and its polycyanurate in the smallest pores. The  $T_g$  values are designated as a primary  $T_{g1}$ , which is generally depressed relative to the bulk, and a secondary  $T_{g2}$  which occurs at higher temperatures and is generally associated with more constrained material in the vicinity of the pore wall [4,13,14,22,29–39]; the designation is a result of the magnitude of the step change in heat capacity at  $T_g$ , with the primary value showing a larger step in  $C_p$  (at least at the larger pore sizes). In Fig. 2, the change in primary  $T_{g1}$  is shown as filled symbols. The changes in  $T_{g1}$  for the monocyanate ester and dicyanate ester are small, on the order of just a few degrees K at the smallest pore sizes, whereas the changes in primary  $T_g$  of the cyanurate is significantly larger, on the order of 30 K for 8.1 nm pores, and that of the polycyanurate network is the largest showing a 50 K depression at 11.5 nm. The depressed  $T_g$  in the polycyanurate system also appears to be nonlinear; this trend, which was pointed out by Alcoutlabi and McKenna in their recent review [3], may arise from the fact that two  $T_g$ s are observed in this material for the smallest 11.5 nm pores, whereas only one  $T_g$  is observed in the 24.6 nm pores – thus, these  $T_g$  values do not necessarily reflect relaxation of the same material. Backing up this assertion is the fact that in native pores, two  $T_g$ s are observed at both of these pore sizes and a monotonic decrease in  $T_{g1}$  with reciprocal pore size is observed. [14]

It is clear that the depressions are significantly greater in the higher molecular weight cyanurate ( $M_n = 712$  g/mol) and in the crosslinked polycyanurate network ( $M_n = \infty$ ). It has been suggested that the magnitude of the  $T_g$  depression at a given confinement size can be tuned by modification of the molecular structure [40,41] or addition of diluent [42] presumably through the changes in the size of the cooperatively rearranging region (CRR) [40,42] or in chain stiffness [41]. For our system of materials, chain stiffness is perhaps not appropriate since three of the materials are not chains, and in previous work on polycyanurate, [14] changes in the size of the CRR did not seem to correlate with the  $T_g$  depression. Rather, in our case, the  $T_g$  depression seems to be roughly related to molecular size and to the bulk  $T_g$  of the four materials studied:  $T_{g, \text{bulk}} = -60.3^\circ\text{C}$  for monocyanate ester,  $-27.4^\circ\text{C}$  for dicyanate ester,  $46.8^\circ\text{C}$  for cyanurate, and  $198.0^\circ\text{C}$  for polycyanurate. The bulk  $T_g$  also inversely reflects the configurational entropy or free volume of the material. A similar result was found when conversion was changed in the dicyanate ester system, with increasing conversion resulting in a decrease in entropy, an increase in chain stiffness, and larger nanoconfinement effects (i.e., larger depressions in  $T_g$ ). [14]

On the other hand, the secondary  $T_g$  appears to mirror the primary  $T_g$ , as shown by the open symbols in Fig. 2; the difference between the two  $T_g$ s appears to be independent of molecular weight in this system of materials and to only increase slightly with decreasing pore size. Reanalysis of data from Park and McKenna [4] also show that the difference  $T_{g2} - T_{g1}$  in that work is nearly independent of concentration in a series of polystyrene/OTP solutions of different polymer concentration; their data also shows a slight increase in the difference ( $T_{g2} - T_{g1}$ ) as pore size decreases.

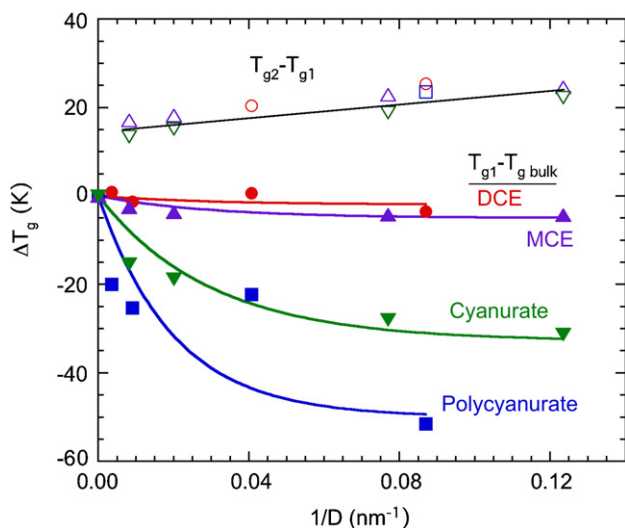


**Fig. 2.** Change in  $T_g$  versus reciprocal pore diameter. Filled symbols give the change in the primary  $T_g$  from the bulk ( $T_{g1} - T_{g, \text{bulk}}$ ). Open symbols show the difference between secondary and primary  $T_g$ s ( $T_{g2} - T_{g1}$ ). Symbols are as follows: ( $\blacktriangle$ ,  $\triangle$ ) monocyanate ester (MCE); ( $\bullet$ ,  $\circ$ ) dicyanate ester (DCE); ( $\blacktriangledown$ ,  $\triangledown$ ) cyanurate; ( $\blacksquare$ ,  $\square$ ) polycyanurate. Lines are a guide to the eye only. View in color for better clarity.

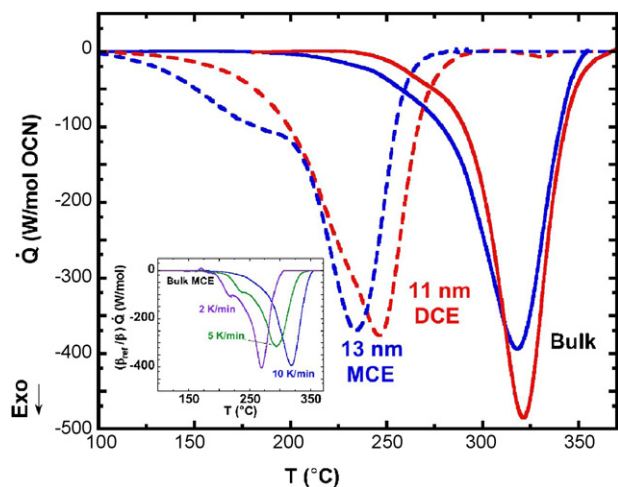


**Fig. 3.** Representative heat flow versus temperature on heating at 10 K/min. Initially unreacted material in bulk is shown as solid curves and nanoconfined material is shown as dashed curves: blue, monocyanate ester (MCE); red, dicyanate ester (DCE). The inset shows heat flow curves for the bulk MCE at heating rates of 2, 5, and 10 K/min; the curves at 2 and 5 K/min are multiplied by factors of 5 and 2, respectively, so that the area of all curves are comparable. View in color for better clarity.

### 3.2. Effect of pore size on the cure kinetics of cyanate ester

The cure kinetics of the mono- and di-cyanate esters in bulk and nanoconfined in controlled pore glasses are investigated by analysis of the DSC reaction exotherms obtained from 10 K/min heating scans. Representative heating scans are shown in Fig. 3 for bulk material and for samples nanoconfined to 11.5 and 13.0 nm-diameter pores. The heat flow is reported in W/mol-OCN groups; in this representation, the bulk reactions of mono- and di-functional cyanate esters are very similar, both in terms of heat of reaction, reaction onset temperature, and exotherm shape. Upon nanoconfinement, the heats of reaction do not change within the error of the measurements for either mono- or di-functional cyanate ester being equal to approximately 110 kJ/mol OCN, but the exotherms do move to lower temperatures upon nanoconfinement, indicating increased reactivity. In addition, at the lowest temperatures, a low-temperature shoulder appears in the exotherms. Since this shoulder appears also in bulk material at low heating rates, as shown in the inset in Fig. 1 for bulk monofunctional cyanate ester, it is attributable to the complex trimerization reaction mechanism [43] and not to inherent changes in the mechanism upon nanoconfinement. However, it should be noted that the second-order plus second-order autocatalytic reaction model derived from the complex mechanism to describe isothermal curing data [43] cannot capture the low-temperature shoulder although it contains two activation energies.

In order to quantify the reaction acceleration associated with the movement of the exotherms to lower temperatures, we convert the temperature axis to a time axis using the apparent activation energy:

$$t_{\text{ref}} = \frac{1}{\beta} \int e^{-\frac{E}{R} \left( \frac{1}{T} - \frac{1}{T_{\text{ref}}} \right)} dT \quad (1)$$

where  $t_{\text{ref}}$  is the isothermal time at a given reference temperature ( $T_{\text{ref}} = 100^\circ\text{C}$  in this work) that would be required to obtain the same degree of reaction as had occurred during the heating scan to temperature  $T$ .  $\beta$  is the heating rate. The apparent activation energy is taken to be 92 kJ/mol (22 kcal/mol), the value obtained in a study of the bulk cure kinetics of dicyanate ester. [43] The activation energy is not expected to differ significantly between the mono- and di-

functional cyanate esters; this assumption is backed up by the similarity of the two exotherms shown in Fig. 3. In addition, analysis of heating scans taken at different rates using an isoconversion methodology similar to those used by Vyazovkin [44] indicates that the activation energies for both the bulk and nanoconfined monocyanate ester are the same within the error of the measurements and also that they are similar to the value obtained in the earlier work on dicyanate ester. At the lowest conversions (below  $\sim 20\%$ ), there is some indication that the activation energy may decrease by approximately 10%, but it is not clear that the decrease is statistically significant. Hence, for ease of analysis, we will assume constant activation energy over the entire range of conversions.

As mentioned, the temperature axis of the dynamic temperature scans is converted to time using Eq. (1). On the other hand, the partial area of the heat flow exotherm can be converted to conversion using the total heat of reaction ( $\Delta H_T$ ):

$$x = \frac{1}{\Delta H_T} \int_{T_0}^T \frac{\dot{Q}}{\beta} dT \quad (2)$$

where  $\beta$  is the heating rate (10 K/min),  $\dot{Q}$  is the rate of heat flow after baseline subtraction, and  $T_0$  is the temperature where the exotherm first deviates from the baseline. Fig. 4 shows the result of the analysis for three replicate runs of monocyanate ester in the 8.1, 13.0, 50.0, and 122.1 nm pores, as well as for the bulk. The reaction in the nanopores moves to shorter times given the lower exotherm temperatures observed in the dynamic scans. The degree of acceleration can be quantified by the logarithm of the shift factor ( $\log \alpha$ ) which is needed to shift the response for the nanoconfined samples along the logarithmic time axis to superpose with the bulk response. The curves in Fig. 4 are shown shifted on the right hand side, and they superpose well at all conversions for the largest two pore sizes, but for the smallest pore sizes, the curves superpose well above 30% conversion, but not at lower conversions which correspond to the low temperature shoulder in the exotherms. A similar result is shown in Fig. 5 for the dicyanate ester sample.

The acceleration factor ( $\alpha$ ) is plotted versus reciprocal pore size for the mono- and di-functional cyanate ester samples in Fig. 6. Also shown on the same figure are the acceleration factors obtained from other work [13,14] evaluating the evolution of  $T_g$  during isothermal cure of monocyanate ester at  $142^\circ\text{C}$  and of the dicyanate ester at  $180^\circ\text{C}$ . For the isothermal cure studies, the acceleration factor is taken to be the ratio of the kinetic rate constants for the nanoconfined material and the bulk. In spite of the simplistic assumption of

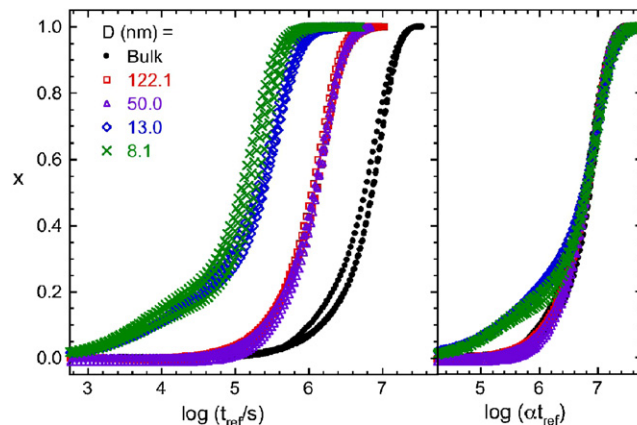


**Fig. 4.** Conversion versus logarithmic time at  $T_{\text{ref}} = 100^\circ\text{C}$ , based on dynamic temperature scans for bulk and nanoconfined monocyanate ester. On the right, the curves are shifted to superpose with the bulk response at the higher conversions. View in color for better clarity.

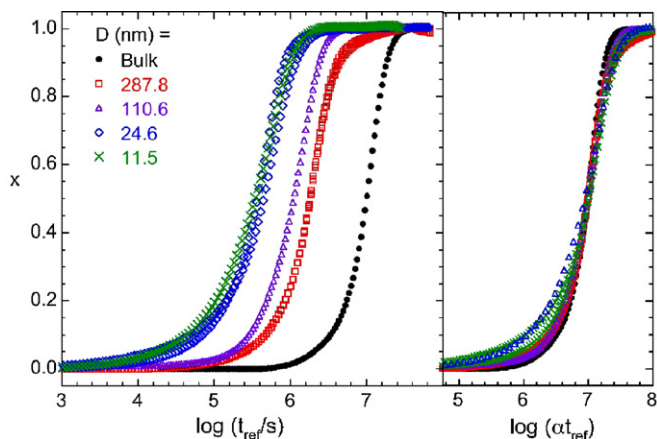


**Fig. 5.** Conversion versus logarithmic time at  $T_{\text{ref}} = 100^\circ\text{C}$ , based on dynamic temperature scans for bulk and nanoconfined dicyanate ester. On the right, the curves are shifted to superpose with the bulk response at intermediate conversions. View in color for better clarity.

constant activation energy, there is reasonable agreement between the acceleration factors obtained from the isothermal and dynamic curing studies. For the monofunctional cyanate ester, the acceleration factor at the smallest pore size of 8.1 nm is  $43 \pm 11$  based on the dynamic data, whereas it is approximately  $20 \pm 1$  based on analysis of both the  $T_{g1}$  and  $T_{g2}$  isothermal data. A similar difference was found for monofunctional cyanate ester in the 13.0 nm pores. For the difunctional cyanate ester in the smallest 11.5 nm pores, on the other hand, the acceleration constant is 26.3 from the dynamic scan and  $19.5 \pm 6.5$  and  $28.6 \pm 19.8$  for the isothermal evolution of  $T_{g1}$  and  $T_{g2}$ , respectively.

The acceleration factors for the monocyanate ester from the dynamic scans are approximately twice those from the isothermal studies, whereas the two sets of data give more similar results in the case of the dicyanate ester. It is not clear why this is the case, although it could be due in part to the appearance of the low temperature shoulder in the dynamic temperature scans, which is much more apparent for the monocyanate ester confined to the smallest pores. In fact, analysis of the data to obtain an acceleration factor at 10% conversion gives  $\log \alpha = 2.3 \pm 0.3$  for monofunctional cyanate

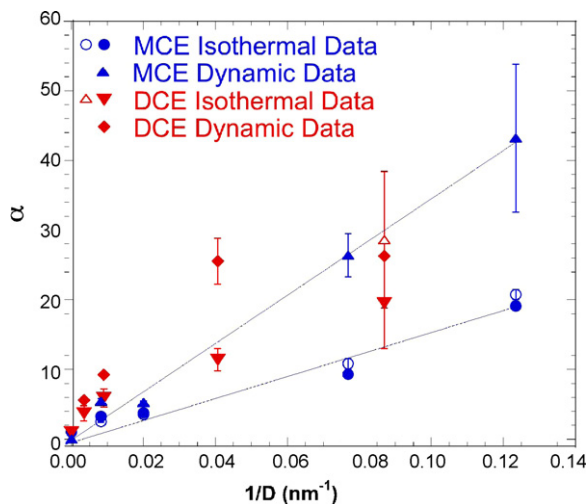


**Fig. 6.** Reaction acceleration factor,  $\alpha$ , versus reciprocal nanopore diameter from isothermal and dynamic studies of monocyanate ester (MCE) and dicyanate ester (DCE). For the isothermal studies, filled symbols indicate the results for the primary  $T_g$  and open symbol are those for the secondary  $T_g$ . Lines are a guide to the eye only. View in color for better clarity.

ester in the 8.1 nm pores and gives  $\log \alpha = 1.9$  for difunctional cyanate ester in the 11.5 nm pores – both values are significantly higher than those obtained by shifting the data at higher conversions and are greater than the values from isothermal scans. Nevertheless, it is apparent that the trimerization reaction is similarly accelerated for both mono- and di-functional reactants. Consequently, we can conclude that the monomer cyclization side reaction, which can occur in the reaction of dicyanate ester but not in the monocyanate ester trimerization, is not responsible for the acceleration of the reaction. The acceleration is also not inherent to other aspects associated with polymerization of the dicyanate ester since the monocyanate ester forms only the low molecular weight cyanurate trimer as product.

Finally, a comment is warranted concerning analysis of isothermal versus dynamic data. In our previous works, [13,14] we obtained  $T_g$  and conversion as a function of time of isothermal cure and performed a kinetic analysis to obtain the acceleration factor. Such data is time-consuming to obtain because quite a number of samples, each cured isothermally for specific times ranging from 10 min to several days, are needed to obtain  $T_g$  and conversion versus cure time over the entire conversion range. On the other hand, dynamic scans are easily obtained in a matter of minutes or hours, depending on the heating rate. The disadvantage of the dynamic scans, however, is that if quantification of changes in reaction rate are to be made, it is necessary to make assumptions concerning the overall activation energy, as we have done in this work. A second disadvantage is that changes in reactivity are observed by shifts of the exothermic reaction to different temperature ranges – hence, a second assumption must be made concerning the invariance (or near invariance) of the reaction mechanism over a wide range of temperatures. These disadvantages should not be underestimated, but as was shown in this work, reasonable agreement between the acceleration factor from the dynamic and isothermal studies can be obtained.

#### 4. Conclusions

The  $T_g$  depression of monocyanate ester, dicyanate ester, and their respective reaction products, cyanurate and a polycyanurate network, are compared as a function of nanopore confinement size. The two reactants show only a few degrees depression in the smallest pore sizes (8.1 nm for monocyanate ester and 11.5 nm for dicyanate ester), whereas the cyanurate shows a 30 K depression at 8.1 nm and the polycyanurate network shows a 50 K depression at 11.5 nm. Perhaps more remarkable, the trimerization reaction of cyanate ester is accelerated in the nanopores. This can clearly be observed from a shift in the reaction exotherms to lower temperatures as pore size decreases. The acceleration is quantified by converting the temperature axis to time assuming a constant activation to obtain conversion versus time and then using time-pore size superposition to shift the curves to the bulk response. The reaction acceleration thus obtained from the dynamic temperature scans is in reasonable agreement with that obtained from isothermal cure studies. The acceleration factor for the monocyanate ester reaction is  $43 \pm 11$  in 8.1 nm pores (compared to a value of  $20 \pm 1$  from isothermal studies), whereas the acceleration for the dicyanate ester is 26.3 in 11.5 nm pores (compared to the values of  $19.5 \pm 6.5$  and  $28.6 \pm 9.8$  from the isothermal studies based on  $T_{g1}$  and  $T_{g2}$ , respectively.) Significantly higher acceleration factors appear to be obtained if the data is analyzed at low conversions.

#### Acknowledgements

The authors would like to acknowledge the American Chemical Society Petroleum Research Fund grant number 45416-AC7, the National Science Foundation grant CMMI-0826437, and the Texas

Higher Education Coordinating Board Advanced Research Program for their financial support of various parts of this project. The donation of part of the controlled pore glasses from Millipore is also gratefully acknowledged.

## References

- [1] C.L. Jackson, G.B. McKenna, *J. Chem. Phys.* 93 (1990) 9002.
- [2] C.L. Jackson, G.B. McKenna, *J. Non-Cryst. Solids* 131–133 (1991) 221.
- [3] M. Alcoutlabi, G.B. McKenna, *J. Phys. Condens. Matter* 17 (2005) R461.
- [4] J.-Y. Park, G.B. McKenna, *Phys. Rev. B* 61 (2000) 6667.
- [5] J. Zhang, G. Liu, J.J. Jonas, *Phys. Chem.* 96 (1992) 3478.
- [6] C.L. Jackson, G.B. McKenna, *Chem. Mater.* 8 (1996) 2128.
- [7] J.S. Sharp, J.H. Teichroeb, J.A. Forrest, *Eur. Phys. J. E* 15 (2004) 473.
- [8] Z. Fakhraai, J.S. Sharp, J.A. Forrest, *J. Poly. Sci. Part B: Polym. Phys.* 42 (2004) 4503.
- [9] H.K. Christenson, *J. Phys. Condens. Matter* 13 (2001) R95.
- [10] C. Alba-Simionesco, B. Coasne, G. Dosse, G. Dudziak, K.E. Gubbins, R. Radhakrishnan, M. Sliwinska-Bartkowiak, *J. Phys. Condens. Matter* 18 (2006) R15.
- [11] K. Dalnoki-Veress, J.A. Forrest, C. Murray, C. Gigault, J.R. Dutcher, *Phys. Rev. E* 63 (2002) 031801.
- [12] A. Schönhals, H. Goring, C. Schick, *J. Non-Cryst. Solids* 305 (2002) 140.
- [13] Q.X. Li, S.L. Simon, *Macromolecules* 41 (2008) 1310.
- [14] Q.X. Li, S.L. Simon, *Macromolecules* 42 (2009) 3573.
- [15] F.W. Starr, T.B. Schroder, S.C. Glotzer, *Phys. Rev. E* 64 (2001) 021802.
- [16] A. Bansal, H. Yang, C. Li, K. Cho, B.C. Benicewicz, S.K. Kumar, L.S. Schadler, *Nature Mater.* 4 (2005) 693.
- [17] A. Bansal, H. Yang, C. Li, B.C. Benicewicz, S.K. Kumar, L.S. Schadler, *J. Polym. Sci. Part B: Polym. Phys.* 44 (2006) 2944.
- [18] P. Rittigstein, J.M. Torkelson, *J. Polym. Sci. B: Polym. Phys.* 44 (2006) 2935.
- [19] J.M. Kropka, V. Pryamitsyn, V. Ganesan, *Phys. Rev. Lett.* 101 (2008) 075702.
- [20] V. Erb, diploma thesis, Max-Planck-Institut für Polymerforschung, Mainz, 1993.
- [21] P. Huber, S. Gruner, C. Schafer, K. Knorr, A.V. Kityk, *Eur. Phys. J. Special Top.* 141 (2007) 101.
- [22] W. Zheng, S.L. Simon, *J. Chem. Phys.* 127 (2007) 194501.
- [23] M.A. DeBolt, A.J. Easteal, P.B. Macedo, C.T. Moynihan, *J. Am. Ceram. Soc.* 59 (1976) 16.
- [24] C.T. Moynihan, P.B. Macedo, C.J. Montrose, P.K. Gupta, M.A. DeBolt, J.F. Dill, B.E. Dom, P.W. Drake, A.J. Easteal, P.B. Elterman, R.P. Moeller, H. Sasabe, J.A. Wilder, *Ann. NY Acad. Sci.* 279 (1976) 15.
- [25] P. Badrinarayanan, W. Zheng, Q.X. Li, S.L. Simon, *J. Non-Cryst. Solids* 353 (2007) 2603.
- [26] C.T. Moynihan, A.J. Easteal, M.A. DeBolt, J. Tucker, *J. Am. Ceram. Soc.* 59 (1976) 12.
- [27] D.J. Plazek, Z.N. Frund, *J. Poly. Sci. Part B: Polym. Phys.* 28 (1990) 431.
- [28] S.D. Kim, J.M. Torkelson, *Macromolecules* 35 (2002) 5943.
- [29] M. Arndt, R. Stannarius, W. Gorbatschow, F. Kremer, *Phys. Rev. E* 54 (1996) 5377.
- [30] M. Arndt, R. Stannarius, H. Groothues, E. Hempel, F. Kremer, *Phys. Rev. Lett.* 79 (1997) 2077.
- [31] G. Barut, P. Pissis, R. Pelster, G. Nimtz, *Phys. Rev. Lett.* 80 (1998) 3543.
- [32] Y.B. Mel'nichenko, J. Schüller, R. Richert, B. Ewen, C.-K. Loong, *J. Chem. Phys.* 103 (1995) 2016.
- [33] P. Pissis, A. Kyritsis, G. Barut, R. Pelster, G. Nimtz, *J. Non-Cryst. Solids* 235–237 (1998) 444.
- [34] P. Pissis, A. Kyritsis, D. Daoukaki, G. Barut, R. Pelster, G. Nimtz, *J. Phys. Condens. Matter* 10 (1998) 6205.
- [35] A. Schönhals, H. Goering, C. Schick, B. Frick, R. Zorn, *Colloid Polym. Sci.* 282 (2004) 882.
- [36] J. Schüller, Y.B. Mel'nichenko, R. Richert, E.W. Fischer, *Phys. Rev. Lett.* 73 (1994) 2224.
- [37] J. Schüller, R. Richert, E.W. Fischer, *Phys. Rev. B* 52 (1995) 15232.
- [38] A. Patkowski, T. Ruths, E.W. Fischer, *Phys. Rev. E* 67 (2003) 021501.
- [39] C. Streck, Y.B. Mel'nichenko, R. Richert, *Phys. Rev. B* 53 (1996) 5341.
- [40] C.G. Campbell, B.D. Vogt, *Polymer* 48 (2007) 7169.
- [41] C.J. Ellison, M.K. Mundra, J.M. Torkelson, *Macromolecules* 38 (2005) 1767.
- [42] C.J. Ellison, R.L. Ruzskowski, N.J. Fredin, J.M. Torkelson, *Phys. Rev. Lett.* 92 (2004) 095702.
- [43] S.L. Simon, J.K. Gillham, *J. Appl. Polym. Sci.* 47 (1993) 461.
- [44] S. Vyazovkin, *J. Comput. Chem.* 18 (1997) 393.